Journal of Energy and Power Engineering 8 (2014) 973-980

Revisiting Stainless Steel as PWR Fuel Rod Cladding after Fukushima Daiichi Accident

Alfredo Abe[1], Claudia Giovedi[2], Daniel de Souza Gomes[1] and Antonio Teixeira e Silva[1]

1. Nuclear Engineering Center, Nuclear and Energy Research Institute, Brazilian Nuclear Energy Commission, São Paulo 05508-000, Brazil

2. Laboratory for Developing of Nuclear Fuel and Instrumentation, Navy Technological Center, São Paulo 05508-000, Brazil

Received: December 03, 2013 / Accepted: January 23, 2014 / Published: June 30, 2014.

Abstract: In the past, stainless steel was utilized as cladding in many PWRs (pressurized water reactors), and its performance under irradiation was excellent. However, stainless steel was replaced by zirconium-based alloy as cladding material mainly due to its lower neutron absorption cross section. Now, stainless steel cladding appears as a possible solution for safety problems related to hydrogen production and explosion as occurred in Fukushima Daiichi accident. The aim of this paper is to discuss the steady-state irradiation performance using stainless steel as cladding. The results show that stainless steel rods display higher fuel temperatures and wider pellet-cladding gaps than Zircaloy rods and no gap closure. The thermal performance of the two rods is very similar and the neutron absorption penalty due to stainless steel use could be compensating by combining small increase in U-235 enrichment and pitch size changes.

Key words: Austenitic stainless steel cladding, Zircaloy cladding, PWR fuel rod, steady-state fuel performance codes.

1. Introduction

The immediate cause of the March 2011 accident at Fukushima Daiichi nuclear power plant was the melting of the reactor core. During this process, the zirconium of the fuel cladding reacted with the water, producing a large amount of hydrogen. This hydrogen, combined with the volatile radioactive materials, leaked out of the containment vessels and entered into the reactor buildings, resulting in explosions. The use of stainless steel cladding has the advantage of not presenting the violent oxidation reaction that occurs with zirconium-based alloys at high temperatures. During the Fukushima Daiichi accident [1], this reaction caused the release of large amounts of hydrogen and major structural damage to the reactor core structure.

Corresponding author: Claudia Giovedi, Ph.D., researcher, research fields: fuel performance and design. E-mail: claudia.giovedi@ctmsp.mar.mil.br.

Austenitic stainless steel was the chosen material for fuel rod cladding in the first PWRs (pressurized water reactors). Since 1960 stainless steel claddings have been replaced in commercial reactor cores by zirconium-based alloys, due to its lower absorption cross section for thermal neutrons and its higher melting temperature. This lower absorption for thermal neutrons allows cores using zirconium-based alloys as fuel rod cladding to operate with lower enrichment cost than cores using stainless steel as cladding material.

Despite the above factors, there are some benefits in using stainless steel as cladding material in PWRs. During steady-state and controlled transients, austenitic stainless steel is more resistant than Zircaloy and is therefore less susceptible to damage due to PCMI (pellet cladding mechanical interaction). Stainless steel is also less susceptible than Zircaloy to stress corrosion cracking generated by fission products in the fuel. As a result, the formation of cracks on the cladding inner wall is less likely and higher

concentrations of fission products can be tolerated in stainless steel fuel rods. During LOCA (loss of coolant accidents), in which the cladding temperatures remain below 1,200 °C, austenitic stainless steel exhibits a metal-vapor reaction rate, a quantity of liberated hydrogen and a reaction heat lower than Zircaloy. The potential for oxygen embrittlement is almost inexistent for stainless steel and its mechanical strength and ductility are better than those of Zircaloy. This results in a smaller cladding deformation and reduced cooling channel blockage.

The austenitic stainless steels used as fuel rod cladding in the first PWRs were of types AISI 304, 347 and 348. With the exception of small isolated failures, its performance was excellent. Nevertheless, only limited efforts have been made to model the thermal-mechanical behavior of PWR fuel rod using stainless steel as cladding.

In recent years, detailed investigations of the interrelated effects of the fuel rod thermal-mechanical behavior under irradiation have been carried out by fuel performance codes. Of all the available codes, only FCODE-BETA/SS [2] could model the steady-state behavior of PWR fuel rod using stainless steel as cladding. Due to the proprietary nature of this code, a group of IPEN-CNEN/SP researchers concluded that efforts should be applied in the construction of a fuel performance code to model the thermal-mechanical behavior of PWR fuel rod using stainless steel as cladding and a particular emphasis was given for type AISI 348. The basis for this new code was the FRAPCON-3.4 code [3] sponsored by U.S.NRC (the United States Nuclear Regulatory Commission) for the licensing of nuclear power plants. Since this code is restricted to evaluate zirconium-based alloys cladding, it was modified to evaluate stainless steel as cladding.

This paper presents some aspects of the PWR steady-state stainless steel cladding fuel behavior under irradiation. Section 2 describes the construction of the code IPEN-CNEN/SS. Section 3 presents the code IPEN-CNEN/SP simulation results for the thermal-mechanical irradiation behavior of type 348 stainless steel cladding and the comparison between these results and those obtained from the code FRAPCON 3.4 simulation using Zircaloy-4 as cladding considering the same geometry and characteristics under the same power history.

2. Construction of IPEN-CNEN/SS

Reliable prediction of fuel rod steady-state behavior constitutes a basic demand for safety calculations, design purposes and fuel performance assessments. Due to the large number of interacting physical, chemical and thermo-mechanical phenomena occurring in a fuel rod during irradiation, it is necessary to perform calculations using computer codes. These codes permit to evaluate the variation as function of time of all significant fuel rod variables, including fuel and cladding temperatures, cladding stress and strain, cladding oxidation, fuel irradiation swelling, fission gas release, and rod internal gas pressure. FRAPCON-3.4 uses fuel, cladding, and gas material properties from MATPRO [4] that was updated to include burnup-dependent properties and properties for advanced zirconium-based alloys. In conventional power reactors, the fuel rod consists of UO_2 pellets inside a zirconium-based alloy cladding called Zircaloy-2 (Zr-98%; Sn-1.5%; Fe-0.15%; Cr-0.1%; Ni-0.05%) used in BWR (boiling water reactors) and Zircaloy-4 (with removal of Ni), where the Ni is removed, used in pressurized water reactors (PWR and CANDU (Canada Deuterium Uranium)). To be used as cladding, there are also the advanced alloys modified with addition of niobium replacing the zirconium (Nb-1%; Zr) such as ZIRLO and M5. The main advantage related to the modified zirconium-based alloys ZIRLO and M5 is the higher corrosion resistance compared to the original Zicaloy-2 and Zircaloy-4.

In order to evaluate the steady-state irradiation performance of stainless steel cladding, it is necessary to include the mechanical and physics properties of austenitic stainless steel in the fuel performance codes.

In nuclear applications, the intergranular corrosion resistant stainless steels, such as AISI 321, 347 and 348 are more suitable. The type AISI 348 presents in its composition, in percent by weight, the following elements: (Fe-balance, C-0.08%, Mn-2.00%, Si-1%, Cr-17 to 19%, Ni-9 to 13%, P-0.045%, S-0.03%, Cu-0.2%, Nb-0.7%, Ta-0.1%, Co-0.2%). The low carbon content associated with the addition of tantalum and niobium prevent corrosion and intergranular precipitation of metallic carbide, $M_{26}C_6$ type, in the region of grain boundaries, avoiding depletion of chromium.

The distinctions between the irradiation performance of stainless steel and Zircaloy claddings can be verified by comparing the properties of these materials. The main properties are summarized in Table 1.

The type 348 stainless steel displays a higher thermal conductivity. Also, it presents a thermal expansion coefficient approximately three times higher than that of Zircaloy-4. Due to this last aspect, stainless steel rods maintain a wider pellet-cladding gap and it is necessary longer irradiation times to verify gap closure than Zircaloy-4 rods. Zircaloy-4 creep deformations result from the combination of irradiation creep and thermal creep, which under steady state operating condition are of the same order of magnitude. For stainless steel rods under the same conditions only irradiation creep is significant. On the other hand, Zircaloy-4 creep rate can be about four times higher than that of type 348 stainless steel creep rate. Under steady-state operating condition Zircaloy-4 is highly resistant to void swelling, but exhibits a substantial axial growth. Unlike Zircaloy-4, type 348 stainless steel has no anisotropic growth but is susceptible to void swelling. Type 348 stainless steel presents an elastic modulus higher than Zircaloy-4 resulting that during PCMI, the cladding deformations will be significantly smaller when compared to those of the Zircaloy-4 cladding. Table 2 shows the MATPRO Zircaloy cladding material properties modified to construct IPEN-CNEN/SS.

Table 1 Zircaloy-4 [5, 6] and type 348 austenitic stainless steel properties [7-9].

Property	Zircaloy-4	AISI 348
Crystalline structure	HCP(α)/CCC(β)	CFC
Density (10^3 kg/m^3)	6.56	7.84
Rockwell-B hardness	89	85
Ultimate strength (MPa)	413	655
Tensile strength at yield (MPa)	241	275
Maximum elongation (%)	20	45
Elastic modulus (GPa)	99.3	195
Poisson's ratio	0.37	0.27
Shear modulus (GPa)	36	77
Resistivity μ(Ohm.cm)	74	79
Specific heat (J/g·°C)	0.285	0.5
Thermal conductivity (W/mK)	16.8	19.1
Thermal expansion coefficient (10^{-6}/K)	6.7	18.5
Melting point (°C)	1,825	1,400
Under irradiation creep (%) (φ_t = 3.1021 n/cm^2)	0.3	0.045
Capture cross-section (Barn)	$0.184\sigma_c$	$3.13\sigma_c$

3. Comparing the Irradiation Performance of Type 348 Stainless Steel and Zircaloy-4 Claddings under a Common Power History

The steady state irradiation performance of type 348 stainless steel rod was simulated using IPEN-CNEN/SS. The results were compared with those obtained for a Zircaloy rod simulated with FRAPCON-3.4 under the same power history. The main objective was to verify if the differences in the irradiation performance of these rods were consistent with the known differences in the material properties of both cladding materials.

The Zircaloy-4 rod selected for simulation with FRAPCON-3.4 has the characteristics of a typical PWR fuel rod. The same design was used in the simulation with IPEN-CNEN/SS. The stainless steel and the Zircaloy-4 rods were designated, respectively, SS and ZR. Tables 3 and 4 present, respectively, the reactor thermal hydraulics parameters and the fuel rod data used for the fuel performance codes startup.

A cosine axial power distribution was used in the simulations. The fuel rod average LHR (linear heat rating) used in the simulation and the achieved burnup are shown in Fig. 1.

Table 2 Zircaloy cladding material properties modified in MATPRO for the construction of IPEN-CNEN/SS.

Material properties	Modification and reference
Thermal expansion	New model [7, 8]
Thermal conductivity	New model [7, 8]
Elastic modulus	New model [7, 8]
Poison's ratio	New model [7, 8]
Thermal creep	Deleted
Irradiation creep	New model [10, 11]
Axial growth	Deleted
Swelling	New model [10]
Oxidation	Deleted
Pellet-cladding gap Conductance	New emissivity factor [8] and new meyer hardness correlation [12]

Table 3 Reactor thermal hydraulics parameters.

Rated core heat	2,815 MWt
Heat generated in fuel	97.4%
Coolant system pressure	15.5 MPa
Coolant inlet temperature	289.7 °C
Rod linear average power	17.75 kW/m
Coolant mass flux	5,900 kg/s·m^2
Average coolant velocity along the rods	4.97 m/s

Table 4 Fuel rod data for fuel performance code startup.

Parameters	Data
Irradiation time	40,080 h
Cladding outer diameter	9.7 mm
Cladding inner diameter	8.43 mm
Cladding wall thickness	0.635 mm
Cladding roughness	0.000508 mm
Cladding material	Zr-4/348 SS
Fuel pellet diameter	8.25 mm
Fuel stack height	3.81 m
Fuel pellet density	10.41 g/cm^3
Fuel pellet roughness	0.000762 mm
Fuel pellet sintering temperature	1,600 °C
Fuel pellet resinter density change	150 kg/m^3
U-235 enrichment	4.2 %
Plenum length	27.17 cm
Rod internal (He) pressure	2.62 MPa
Fuel rod pitch	1.27 cm

In order to simulate the neutronic behavior of stainless steel and Zircaloy as cladding material, MCNP (monte carlo neutron and particle) code [13] was utilized to obtain the infinite neutron multiplication factor (K_∞). This factor primarily can estimate the neutronic behavior due to different cladding materials.

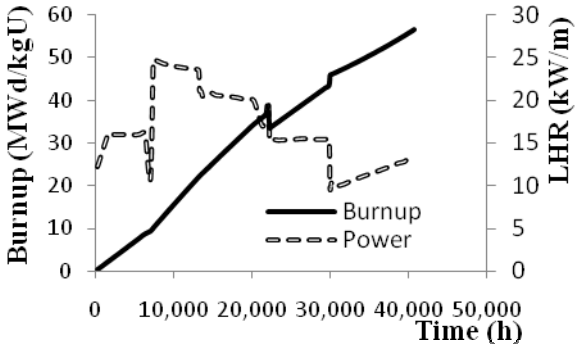

Fig. 1 Fuel rod average linear heat rating (kW/m) and burnup (MWd/kgU).

The difference is directly associated to the material neutron absorption cross section. In this sense, it is well known that one of the reasons to replace stainless steel by zirconium-based alloys was the neutron absorption penalty. The proper parameter to quantify this penalty is the reactivity.

The reactivity parameter (ρ) can be defined as the difference between two different infinite neutron multiplication factors (K_∞), i.e., $\rho = K_\infty$ (zircaloy) – K_∞ (stainless steel). Usually, the meaningful unit of reactivity is expressed as pcm, i.e., $\rho = \Delta K_\infty \times (1.0 \times 10^5)$. So, a representative fuel rod was geometrically modeled according to the data from Table 4 considering UO_2, gap, cladding and moderator regions.

Initially, the MCNP code was used to obtain the infinite neutron multiplication factors for both Zircaloy-4 and stainless steel cladding with the same geometric dimensions (fuel pellet diameter, gap thickness, clad thickness and pitch). Table 5 presents the results of infinite multiplication factor obtained using the MCNP code. The amount of reactivity associated to the cladding is 3,110 pcm. The reactivity obtained subtracting infinite multiplication factors is mainly due to cladding material.

Additionally, the neutronic assessment of the fuel rods allowed determining a new fuel enrichment to

Table 5 Zircaloy-4 and 348 stainless steel infinite neutron multiplication factors.

Fuel rod cladding material	K_∞
Zircaloy-4	1.46062 ± 0.00016
SS-348	1.42952 ± 0.00016

overcome this loss of reactivity due to the higher neutron absorption. This analysis was performed changing only the enrichment parameter in order to match the same infinite multiplication factor value of the previous result for the fuel rod using Zircaloy-4 as cladding material. Taking into account only enrichment as a variable parameter, different MCNP runs were performed to find out the value of infinite multiplication factor. The obtained new enrichment was 4.93% of U-235, representing an increase of approximately 17% compared to the initial enrichment (4.2%). Alternatively, the loss of reactivity can be compensated changing the actual fuel pitch value (distance center to center between two fuel rods) as shown in Table 6.

Nevertheless, changes in the fuel rod pitch should be evaluated properly taking into account other reactor core parameters, such as reactivity coefficients. There is also an alternative of combining enrichment increase with pitch size changes in order to compensate the neutron absorption penalty.

Tables 7 and 8 present, respectively, the data obtained from ZR and SS simulations with, respectively, FRAPCON 3.4 and IPEN-CNEN/SS, including cladding average temperatures, fuel rod gaps, fuel centerline temperatures, contact pressure, hoop stress, fuel outside diameter and rod internal pressures. The evolution under irradiation of ZR and SS gap, fuel outside diameter, fuel centerline temperature, internal pressure and hoop stress are plotted as function of time (Figs. 2-6).

Deviations in the ZR and SS rods behavior at the start of irradiation result from the different thermal expansion coefficients of both materials. As shown in Table 1, type 348 stainless steel exhibits a thermal expansion coefficient higher than Zircaloy-4. The main result of this comparison is that SS maintains a fuel rod gap larger than ZR (Fig. 2) during all irradiation period. Since the gas composition is the same in both fuel rods, rod internal pressure, gap conductance, and fuel temperature are governed mainly by the gap thickness.

Table 6 Infinite neutron multiplication factor as function of fuel rod pitch.

Pitch (cm)	K_∞
1.27	1.42952 ± 0.00016
1.30	1.43843 ± 0.00016
1.36	1.45204 ± 0.00016
1.38	1.45246 ± 0.00016

Fuel centerline temperatures are higher and the gas internal pressure is lower in SS rods (see Table 8). Despite higher fuel temperatures in SS, the average cladding temperatures in SS are lower than in ZR (Tables 7 and 8), due to the fact that SS thermal conductivity is higher than ZR thermal conductivity.

The ZR irradiation creep is of great magnitude. In terms of fuel rod performance, this leads to a large cladding deformation, allowing the ZR gap closure in about 12,000 h (Fig. 2). As stainless steel has an irradiation creep lower than ZR, wider gaps are maintained for a longer time and higher temperatures are achieved in SS rods. No gap closure is verified in the SS rod until the end of the irradiation.

The initial state of compressive stress in the two cladding types (Tables 7 and 8, Fig. 6) is due to the coolant external pressure. The hoop stresses are greater in the SS rod because internal pressure is smaller than ZR rod internal pressure. In the latter, after PCMI in 16,000 h, the hoop stresses alternate between compressive and tensile states until the end of irradiation.

In recent years, the failures that occurred in commercial PWR fuel rods were due mainly to PCMI. PCMI causes deformations and stresses in the cladding that do not reach, in most cases, conditions of mechanical breakdown, but they are sufficient to cause stress corrosion cracking. When the contact occurs, as Zircaloy-4 rigidity is smaller than that of UO_2 pellets, the latter tend to impose a strain on the cladding. However, due to the higher Zircaloy-4 creep, the cladding tends to relax stresses, transforming elastic strains in permanent strains. Consequently, the Zircaloy-4 cladding can undergo large deformations without reaching high stress, but the deformation rates

Table 7 Data obtained from simulation for Zircaloy-4 rod.

	Time (h)	Burnup (MWd/ kgU)	Power (kW/m)	Average cladding temp. (K)	Gap (cm)	Fuel center line temp. (K)	Cont. (MPa)	Hoop stress (MPa)	Fuel outs. diam. (cm)	Internal pressure (MPa)
1	235	0.25	12.17	584	0.00531	922	0	-78.77	0.8335	5.98
2	5,035	6.87	15.91	591	0.00376	1,033	0	-77.85	0.8342	6.14
3	7,373	10.05	24.70	606	0.00216	1,304	0	-72.81	0.8367	6.90
4	9,353	14.20	24.18	606	0.00145	1,276	0	-71.58	0.8372	7.09
5	12,629	20.93	23.62	605	0.00018	1,237	0	-69.09	0.8380	7.49
6	14,069	23.63	20.51	600	0.00013	1,146	0	-69.17	0.8382	7.50
7	16,711	28.32	20.47	600	0.00013	1,168	0	-67.09	0.8374	7.83
8	20,237	34.45	19.95	600	0.00013	1,175	20.22	16.23	0.8371	8.04
9	22,404	33.75	15.42	608	0.00013	1,041	16.73	-7.29	0.8361	7.93
10	25,368	37.67	15.39	609	0.00013	1,052	26.03	55.74	0.8367	7.94
11	28,704	42.10	15.39	609	0.00013	1,065	27.57	66.42	0.8373	8.06
12	30,480	46.43	9.74	591	0.00013	876	9.27	-58.05	0.8371	7.95
13	34,320	49.91	11.09	596	0.00013	929	26.31	58.12	0.8378	8.09
14	37,512	53.14	11.94	599	0.00013	972	32.80	110.79	0.8385	8.23
15	40,080	55.96	13.19	603	0.00013	1,015	33.76	109.49	0.8391	8.36

Table 8 Data obtained from simulation for AISI 348 rod.

	Time (h)	Burnup (MWd/ kgU)	Power (kW/m)	Average cladding temp. (K)	Gap (cm)	Fuel center line temp. (K)	Cont. (MPa)	Hoop stress (MPa)	Fuel outside diam. (cm)	Internal pressure (MPa)
1	235	0.25	12.17	584	0.00650	944	0	-81.88	0.8336	5.52
2	5,035	6.87	15.91	590	0.00582	1,087	0	-81.56	0.8346	5.56
3	7,373	10.05	24.70	604	0.00447	1,408	0	-77.25	0.8375	6.22
4	9,353	14.20	24.18	604	0.00409	1,394	0	-76.51	0.8381	6.33
5	12,629	20.93	23.62	603	0.00340	1,380	0	-75.04	0.8391	6.55
6	14,069	23.63	20.51	598	0.00338	1,266	0	-75.61	0.8388	6.46
7	16,711	28.32	20.47	598	0.00290	1,268	0	-74.38	0.8396	6.65
8	20,237	34.45	19.95	596	0.00231	1,251	0	-72.85	0.8405	6.88
9	22,404	33.75	15.42	602	0.00282	1,107	0	-73.82	0.8391	6.73
10	25,368	37.67	15.39	601	0.00241	1,107	0	-72.61	0.8398	6.92
11	28,704	42.10	15.39	601	0.00196	1,108	0	-70.46	0.8405	7.24
12	30,480	46.43	9.74	587	0.00188	903	0	-72.24	0.8402	6.97
13	34,320	49.91	11.09	590	0.00142	951	0	-69.63	0.8410	7.36
14	37,512	53.14	11.94	593	0.00102	988	0	-67.07	0.8418	7.75
15	40,080	55.96	13.19	595	0.00066	1,021	0	-64.54	0.8424	8.13

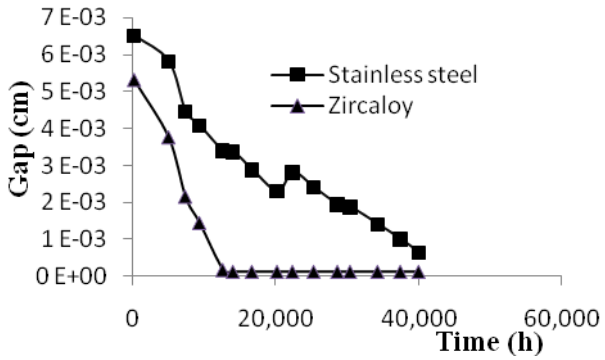

Fig. 2 Pellet-Cladding gaps for ZR and SS rods.

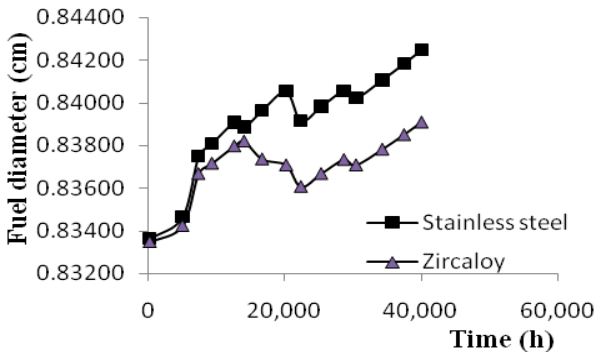

Fig. 3 Fuel outside diameters for ZR and SS rods.

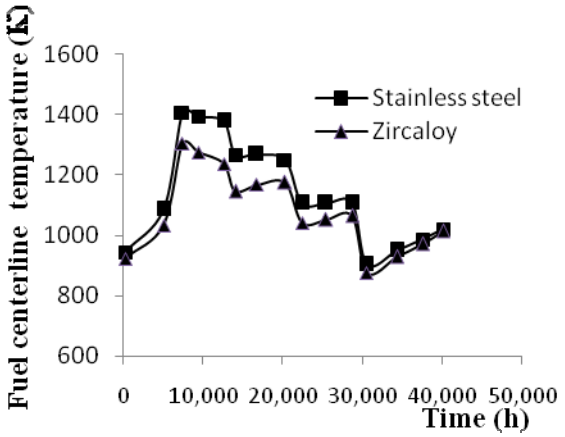

Fig. 4 Fuel centerline temperatures for ZR and SS rods.

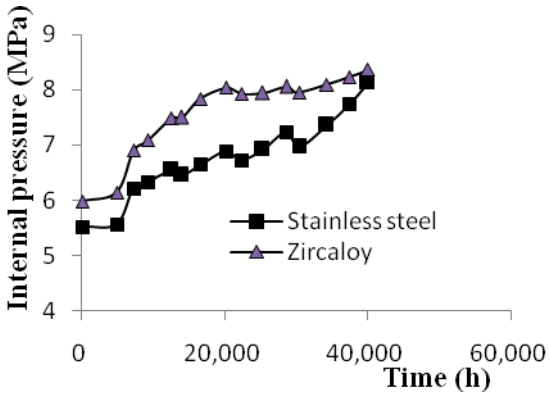

Fig. 5 Internal pressures for ZR and SS rods.

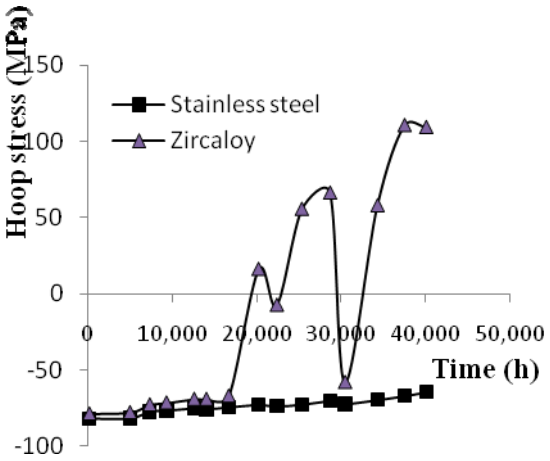

Fig. 6 Hoop stresses for ZR and SS rods.

must be below certain limits in order to not reach the limits for stress corrosion cracking. For stainless steel, its rigidity is of the same order of magnitude of the UO_2 pellets. This implies in a strain competition between the pellets and the cladding during the interaction. In this case it is important to analyze the pellet plastic characteristics as the reaction of the cladding on it is significant [14]. Thus, in case of PCMI, deformations in the stainless steel cladding will be lower than in the ZR cladding, but the stresses achieved will be of the same order or higher in SS rods.

4. Conclusions

Using IPEN-CNEN/SS to compare the performance of type 348 stainless steel and Zircaloy-4 claddings under a common power history reveals that type 348 stainless steel rods display higher fuel temperatures and wider gaps than Zircaloy-4 rods. No gap closure is observed for type 348 stainless steel rod. On the other hand, the Zircaloy-4 cladding spends a high fraction of life in a state of tensile stress at the ridge. Nevertheless, the steady state thermal performance of the two fuel rod types is very similar, confirming that stainless steel could be a good option to replace zirconium-based alloys as cladding material in PWRs in order to improve the safety conditions under accident conditions. Neutronic assessments have shown that the higher stainless steel neutron absorption cross section could be compensated, for the evaluated PWR rod, by increasing about 20% in the U-235 enrichment. Also, there is an alternative of combining enrichment increase with pitch size changes in order to compensate the neutron absorption penalty due to the use of stainless steel.

Thus, the obtained results indicate that stainless steel remains as a possible alternative to be used as cladding in PWRs improving the safety, considering the problems related to hydrogen production and explosion.

Acknowledgments

The authors are grateful to the technical support of IPEN-CNEN/SP and CTMSP (Navy Technological Center).

References

[1] N. Akiyama, H. Sato, K. Naito, Y. Naoi, T. Katsuta, The Fukushima Nuclear Accident and Crisis

Management-Lessons for Japan, U.S. Alliance Cooperation Web site, Sasakawa Peace Foundation, Tokyo, 2012, http://mansfieldfdn.org/blog/the-fukushima-nuclear-accident-and-crisis-management-lessons-for-japan-u-s-alliance-cooperation/.

[2] R.W. Smith, G.S. Was, FCODE-BETA/SS: A fuel performance code for stainless steel clad pressurized water reactor fuel, Nucl. Technol. 69 (2) (1985) 198-209.

[3] K.J. Geelhood, W.G. Luscher, C.E. Beyer, M.E. Flanagan, FRAPCON-3.4: A Computer Code for the Calculation of Steady-State Thermal-Mechanical Behavior of Oxide Fuel Rods for High Burnup, U.S.NRC, NUREG/CR-7022, Washington, 2011.

[4] W.G. Luscher, K.J. Geelhood, M.E. Flanagan, Material Properties Correlations: Comparison between FRAPCON-3.4, FRAPTRAN 1.4, and MATPRO, U.S.NRC, NUREG/CR-7024, Washington, 2011.

[5] C.M. Allison, G.A. Berna, R. Chambers, E.W. Coryell, K.L. Davis, D.L. Hagrman, et al., SCDAP/RELAP5/MOD3.1 Code Manual Volume IV: MATPRO—A Library of Materials Properties for Light-Water-Reactor Accident Analysis, NUREG/CR-6150, EGG-2720, Washington, 1993.

[6] C.C. Busby, Halogen stress corrosion cracking of Zircaloy 4 tubing, J. Nucl. Mate. 55 (1) (1975) 64-82.

[7] TDS-Technical data specification of austenitic stainless steel ATI321/ATI347/ATI348, Allegheny Technologies Incorporated, Pittsburg, USA, 2013.

[8] D. Peckner, I.M. Bernstein, Handbook of Stainless Steels, MacGraw Hill, New York, 1977.

[9] V. Pasupathi, Investigations of Stainless Steel Clad Fuel Rod Failures and Fuel Performance in the Connecticut Yankee Reactor, EPRI 2119, Palo Alto, 1981.

[10] J.M. Beeston, Mechanical and physical properties of irradiated type 348 stainless steel, in: 10th International Symposium on Effects of Radiation on Materials, Savannah, GA, USA, June 5, 1980.

[11] Y. Gorash, Development of a creep-damage model for non-isothermal long-term strength analysis of high temperature components operating ina a wide stress range, Martin Luther University of Halle-Winttenberg, Halle Germany, 2008.

[12] C.E. Beyer, C.R. Hann, D.D. Lanning, F.E. Panisko, L.J. Parchen, GAPCON-THERMAL-2: A Computer Program for Calculating the Thermal Behavior of an Oxide Fuel Rod, BNWL-1898 NRC 1 and 3, Battelle Pacific Northwest Laboratories, Washington, 1975.

[13] MCNP: A General Monte Carlo N-Particle Transport Code, Version 5, LA-UR-03-1987, 2003. (Revised 2/1/2008)

[14] F.G. Basombrio, Simulation of the thermomechanical effects, originated on a fuel pin, with a cracked pellet by different power ramps velocities using a two dimensional finite element model, Nucl. Eng. De. 74 (2) (1983) 247-252.